



## Computational simulation for MEMS combdrive levitation using FEM

Shiang-Woei Chyuan

Chung Shan Institute of Science and Technology, P.O. Box 90008-15-3, Lung-Tan, Tao-Yuan 325, Taiwan, ROC

### ARTICLE INFO

#### Article history:

Received 23 July 2007

Received in revised form 29 March 2008

Accepted 29 March 2008

Available online 8 May 2008

#### Keywords:

MEMS

Levitation

Gap

Traveled distance

FEM

Comb drive

### ABSTRACT

Generally the levitation value is a very important design parameter for a comb drive, because the levitation effect will seriously downgrade the performance and reliability of electrostatic MEMS devices. Thus an accurate electrostatic and structural analysis is essential. Besides the distance traveled by the movable finger of MEMS comb drive, studies of the effect of gap sizes between comb drive fingers and ground plane and between movable and fixed fingers for levitation are also needed. By way of the finite element method, an accurate electrostatic field under diverse gap sizes considering the fringing electric field around the edges of the fixed and movable fingers of comb drive can be obtained. The subsequent levitation and strain analyses for an MEMS comb drive can be also implemented more precisely. Results show that the levitating displacement and strain of the movable finger are dependent on the distance traveled. The smaller the gap between comb drive fingers and ground plane, the larger the structural response of the movable finger. In addition, the levitation also becomes more predominant as the gap between the movable and fixed fingers decreases.

© 2008 Elsevier B.V. All rights reserved.

### 1. Introduction

For MEMS (microelectromechanical systems) comb drive, the resulting electrostatic force drives the movable fingers towards the fixed fingers when a voltage is applied between them. Motion is thereby produced in the direction of the movement of the movable fingers [1,2]. Basically, the in-plane interdigitated comb drives, shown in Fig. 1, are used to produce in-plane and small out-of-plane or torsional motion [3], and the asymmetric comb drives can be utilized to generate large out-of-plane or torsional motion [4]. Generally speaking, investigations of the electric field around the fixed finger, movable finger and ground plane of an MEMS comb drive under diverse gap sizes are very important, since the levitating force acting on the movable finger is clearly dependent on the electrostatic field, especially considering the fringing field around the edges [5]. Among diverse numerical approaches [6,7] in electromagnetics, the finite element method (FEM) [8,9] has become a powerful design tools for engineers due to the increasing development of digital computational power. Besides the FEM, the boundary element method (BEM) is another efficient method, but for problems having degenerate boundary (ill-conditioned) and degenerate scale (rank-deficiency) problems, the conventional BEM cannot be used directly, and we need many external numerical techniques [10,11]. Therefore, the FEM is the most useful and simplest method for the engineer, because there is no laborious artificial boundary technique needed. The FEM is

thus employed and developed to analyze electrostatic and structural problems for MEMS comb drive levitation. After the electrostatic response of the comb finger biased with a DC voltage is accurately calculated, the resulting induced vertical force per unit length exerted on the movable comb finger at different levitation positions can be obtained, and diverse levitations of movable finger under different traveled distances and gap sizes are investigated in detail.

This paper is organized as follows: After the introduction of Section 1, a summary of the procedure for FEM for electrostatic problems is introduced in Section 2. Numerical results are then provided and compared in Section 3 to verify the suitability and accuracy of the FEM. The effects of traveled distance and gap size of MEMS comb drive for the levitation of MEMS comb drive are then studied. Some remarks based on the reported results are discussed in Section 4.

### 2. Finite element modelling for electrostatic problems

From the FEM viewpoint, the formulation of a linear electrostatic problem is appropriately described in matrix form [6–9]:

$$[\mathbf{A}]\{\mathbf{V}\} = \{\mathbf{B}\} \quad (1)$$

where  $\{\mathbf{V}\}$  is the column matrix containing the unknown voltage at nodes,  $\{\mathbf{B}\}$  is the column matrix of voltages at the boundaries, and the band matrix  $[\mathbf{A}]$  is the assemblage of individual element coefficient matrices. In general, Eq. (1) can be solved easily using the Gaussian elimination technique.

E-mail address: [swchyuan@ntu.edu.tw](mailto:swchyuan@ntu.edu.tw)

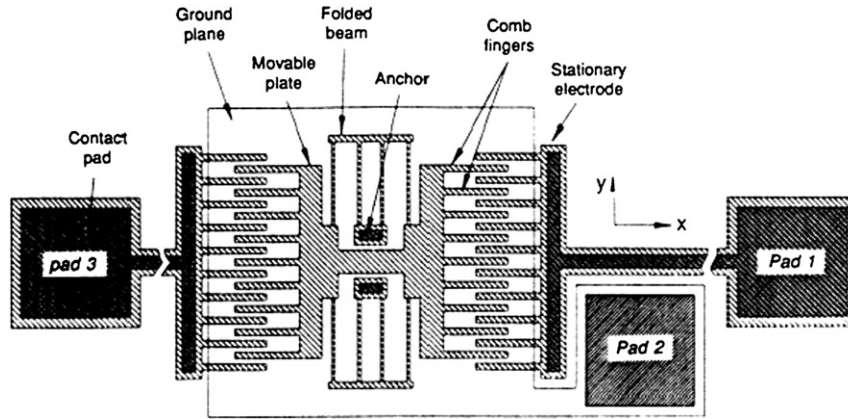


Fig. 1. Layout of a linear lateral resonator driven and sensed with interdigitated capacitors (electrostatic comb drive).

As we know, the electrostatic levitating forces acting on the movable fingers of a comb drive must first be obtained before solving the levitation displacement of MEMS comb drive, hence the electrostatic analysis work to obtain the distribution of surface charge density around the movable finger is the groundwork for calculating the levitating force density. Therefore, choosing an efficient method such as the FEM is necessary for simulating the electric field. In order to calculate accurately the charge distribution ( $\rho_s$ ) on the conductor surfaces of the movable fingers, an FEM analysis has been carried out between the electrostatic and mechanical fields. The two fields are coupled by applying the results for electrostatic (levitating) force from an electrostatic analysis as loads to the structural analysis. The deflection

(levitation) obtained from the structural analysis is then passed back to the electrostatic model, resulting in increased electrostatic forces. This procedure is continued until the change in deflection converges to a very small value.

### 3. Numerical simulation for the levitation of MEMS comb drive

#### 3.1. Case study

A comb finger under levitation force induced by two adjacent electrodes biased at a positive potential  $V_p$  is shown in Fig. 2. In

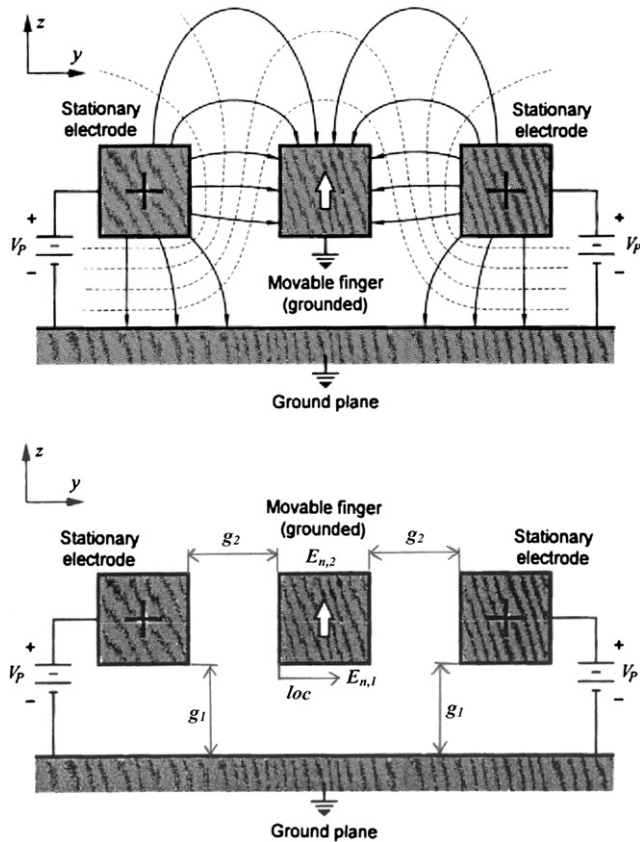


Fig. 2. Cross-section of the potential contours (dashed lines) and the electric fields (solid lines) of a comb finger under levitation force induced by two adjacent electrodes biased at a positive potential.

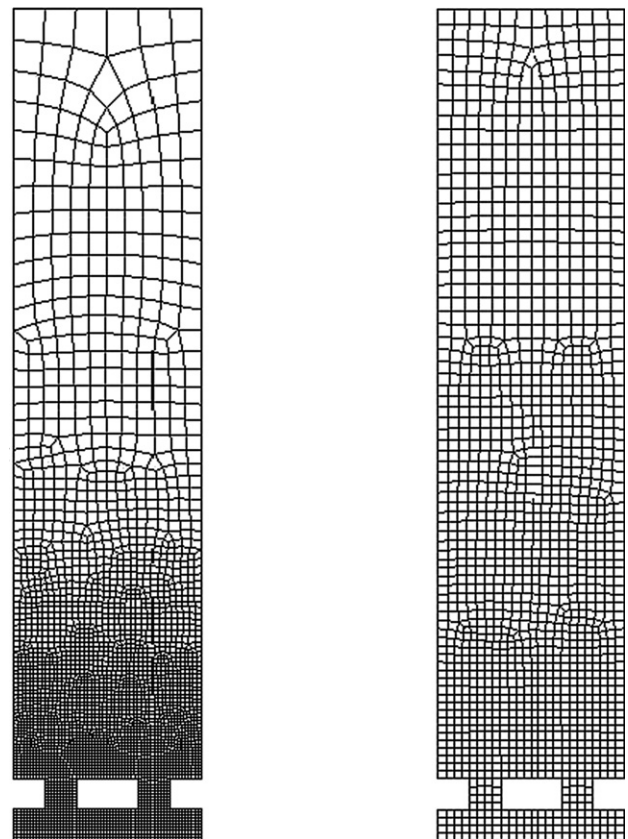


Fig. 3. The related FEM mesh discretization (left part: refined mesh model; right part: coarser mesh model).

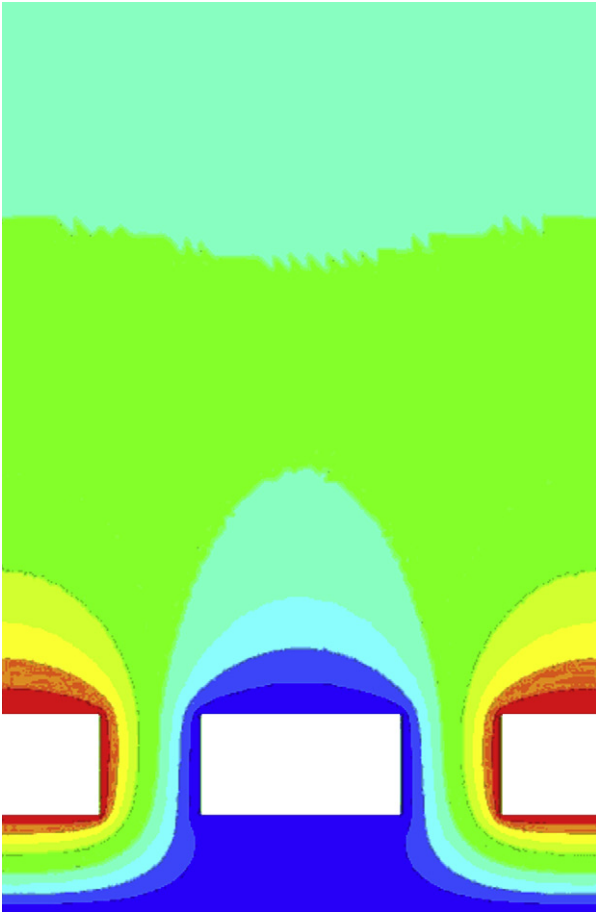


Fig. 4. Results of electric potential field (equipotential lines - - red color: + $V_p$ ; blue color: 0) of comb drive using the refined FEM mesh. [For interpretation of the references to color in this figure legend, the reader is referred to the web version of this article.]

order to check the accuracy of using the FEM, we first determine the electric potential distribution. The effects of gap size between the fingers of a comb drive and ground plane ( $g_1$ ) and that between movable and fixed fingers ( $g_2$ ) on levitating displacement and strain are also investigated.

As noted in Fig. 2, the physical behavior of the electric potential  $V$  and electric field intensity  $E$  of a MEMS comb drive is very complicated, because there is an obvious fringing field around the edges of the fixed and movable fingers. Because it is difficult to obtain an analytical solution, and because simplified numerical models for electrostatic comb drives do not accurately simulate the fringing field [4], the FEM simulation was used. Because of the fringing field around the edges, a refined finite element model was set up in order to obtain a better result. In addition, the symmetric boundary between two adjacent fingers using proper Neumann boundary condition was used to simplify the dimension of FEM model.

Over three thousand nodes will be analyzed using a refined FEM model (3608 elements and 3790 nodes; see Fig. 3a) because the results from the initial FEM model (1490 elements and 1607 nodes; see Fig. 3b) are not adequately accurate. The results of electric potential for the interior nodes between movable and fixed fingers under refined FEM are shown in Fig. 4. By the way of FEM, the distribution of normal electric field intensity ( $E_n$ ) on the bottom and upper side of movable finger can be obtained, respectively. Generally, the values of normal electric field intensity ( $E_{n,1}$ ) on the bottom and that ( $E_{n,2}$ ) on the upper side of movable finger are

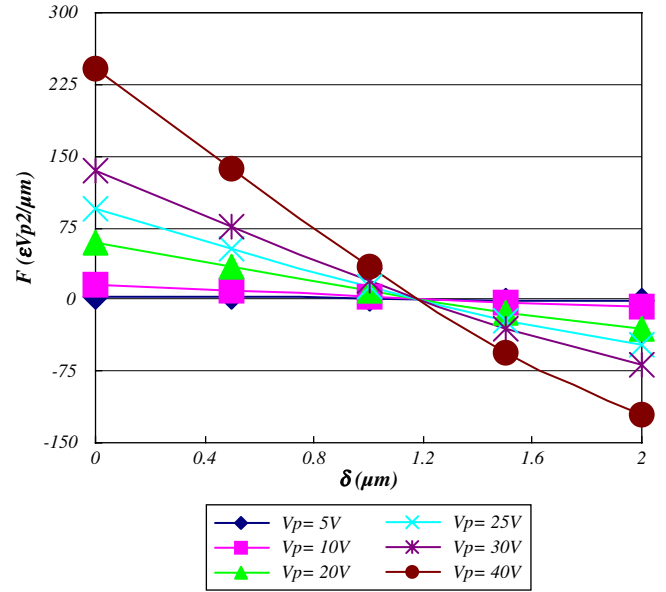


Fig. 5. The levitating force density ( $F$ ) acting on the movable finger under diverse levitation ( $\delta$ ) and  $V_p$ .

obviously dependent on the value of the location to the left side of movable finger ( $loc_y$ ). In addition, the value of  $E_{n,2}$  is higher than that of  $E_{n,1}$  because electric potential gradient, and the values of  $E_n$  near the right and left sides are much higher than those of other region of movable finger due to the fringing effect.

Because the charge distribution on the conductor surfaces can be determined from  $\rho_s = \epsilon E_n$  if  $\epsilon$  is a constant, the relationship between the normal force density  $f_n$  acting on the surface of a conductor and the charge density  $\rho_s$  of that conductor is

$$f_n = -0.5\rho_s^2/\epsilon \tag{2}$$

Thus, the electrostatic force density  $F_n$  acting on the movable finger along the boundary

$$F_n = \int_B f \, dB \tag{3}$$

can be calculated if  $\rho_s$  (or  $E_n$ ) is known. Therefore, the levitating force density  $F$  (normal to the substrate) acting on each movable finger is equal to the resultant of electrostatic force density  $F_n$  between upper side and bottom of concerned movable finger. Because the difference of  $E_{n,1}$  and  $E_{n,2}$  is obvious in this case, the imbalance in the field

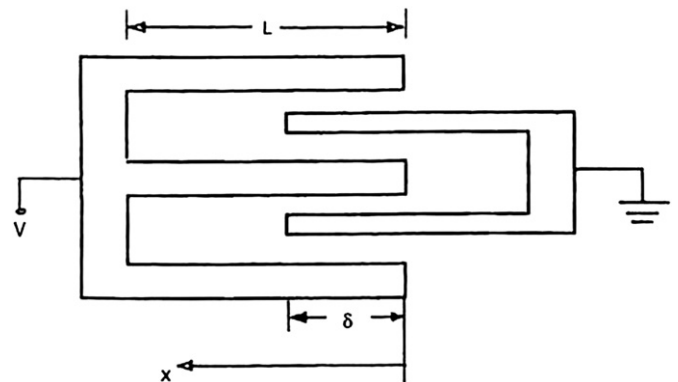


Fig. 6. A typical comb drive with one set of straight fingers.

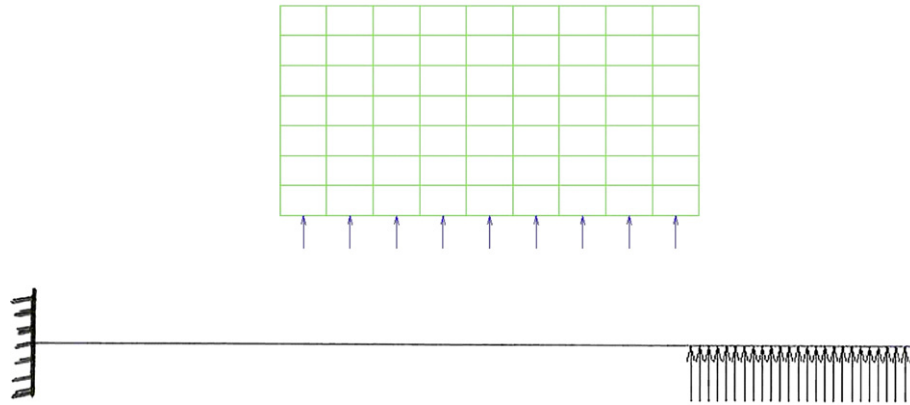


Fig. 7. An illustration of force acting on the movable finger.

distribution will result in a net vertical force induced on the movable comb fingers, which levitates the structure away from the substrate. Calculated by Eqs. (2) and (3), the value of  $F$  is  $0.1504 \epsilon V_p^2 / \mu\text{m}$ . If the values of  $\epsilon$  and  $V_p$  are  $8.854e-12 \text{ F/m}$  and  $20 \text{ V}$ , the value of  $F$  is  $5.3266e-10 \text{ N}/\mu\text{m}$  ( $\approx 5.4353e-8 \text{ Kgf/mm}$ ). To go a step further, the  $F$  under diverse levitation ( $\delta$ ) and  $V_p$  can be shown in Fig. 5. The stable equilibrium levitation,  $\delta_0$ , ( $1.20 \mu\text{m}$  for this case), is the same for any nonzero bias voltages  $V_p$ . Hence, in the absence of a restoring spring force, the movable finger will be levitated to  $\delta_0$  upon the application of a DC bias. Because the value of  $\delta_0$  from Ref. [3] is  $1.22 \mu\text{m}$  for the same case, the difference of  $\delta_0$  between our FEM and Ref. [3] is only 1.64%. Consequently, we can verify the computational accuracy of FEM model implemented in this article.

While the electrostatic analysis is completed, the structural analysis of movable finger under diverse distances traveled by movable finger ( $\delta$ ; see Fig. 6) could be implemented if using domain-type FEM. From the FEM viewpoint, the formulation of a linear elastic static structural problem for solution by the displacement method is appropriately described in the matrix form [8]

$$[\mathbf{K}]\{\mathbf{d}\} = \{\mathbf{P}\} \quad (4)$$

where  $\{\mathbf{d}\}$  is the displacement vector,  $\{\mathbf{P}\}$  is the load vector, and the stiffness matrix  $[\mathbf{K}]$  is given by

$$[\mathbf{K}] = \iiint_V [\mathbf{B}]^T [\mathbf{D}] [\mathbf{B}] dV \quad (5)$$

where matrix  $[\mathbf{D}]$  is the elasticity matrix, and  $[\mathbf{B}]$  is a matrix relating strains and nodal displacements. If the values of Young's modulus  $e$ , Poisson ratio  $\nu$  and length  $L$  of movable finger (polysilicon) are  $150 \text{ GPa}$ . ( $\approx 15 \text{ 306 Kgf/mm}^2$ ),  $0.29$  and  $400 \mu\text{m}$ , respectively, the illustration of force acting on the movable finger is shown in Fig. 7. As we know, the levitating force behaves like an electrostatic spring, so an electrostatic spring (spring constant  $k_z$ ) usually used for levitation control [3]. Solving Eq. (4) using FEM, the numerical values of levitating displacement ( $d_{lev}$ ) and maximum principal strain ( $\epsilon_{max}$ ) are  $1.31 \text{ nm}$  and  $2.47e-6\%$  if the values of  $\delta$ ,  $k_z$  and  $V_p$  are  $20 \mu\text{m}$ ,  $29 \text{ nN}/\mu\text{m}$  ( $\approx 3.06e-6 \text{ Kgf/mm}$ ) and  $1.0 \text{ V}$ , respectively.

Because the gap size between comb drive fingers and ground plane ( $g_1$ ) can play very important role for electrostatic field and levitating force, the study of levitation of movable finger under diverse values  $g_1$  is needed. By way of FEM, the distributions of  $d_{lev}$  and  $\epsilon_{max}$  under diverse values of  $\delta$  and  $g_1$  are shown in Figs. 8 and 9, if the value of  $V_p$  is  $20 \text{ V}$  and the value of gap between movable and fixed fingers ( $g_2$ ) is still confined to  $2.0 \mu\text{m}$ . From the results of Figs. 8 and 9, one can see that the smaller the value of  $g_1$  is, the larger the values of  $d_{lev}$  and  $\epsilon_{max}$  are, and the structural responses of movable

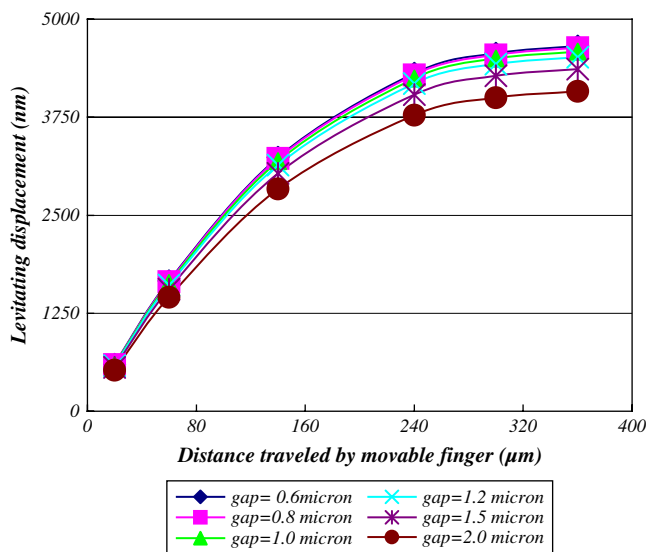


Fig. 8. The distribution of levitating displacement under diverse distances traveled by movable finger and gaps between comb drive fingers and ground ( $V_p = 20 \text{ V}$ ).

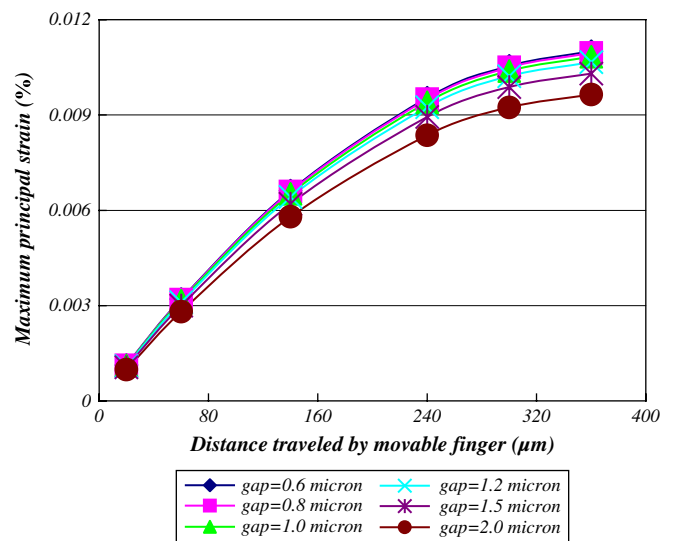
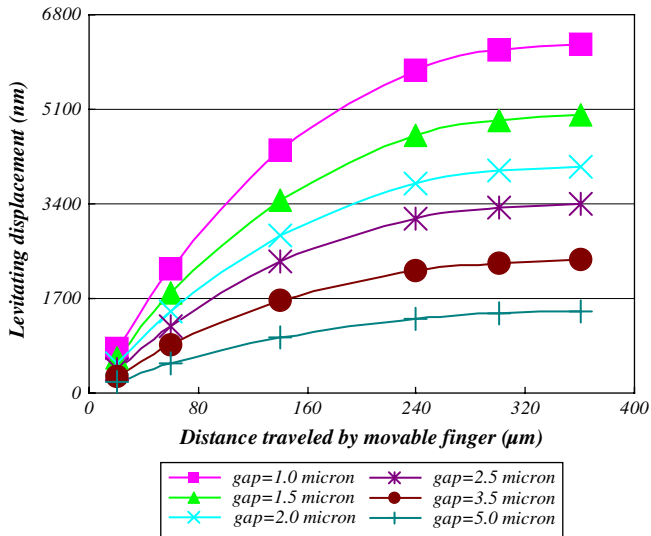


Fig. 9. The distribution of maximum principal strain under diverse distances traveled by movable finger and gaps between comb drive fingers and ground plane ( $V_p = 20 \text{ V}$ ).



**Fig. 10.** The distribution of levitating displacement under diverse distances traveled by movable finger and gaps between movable and fixed fingers ( $V_p = 20$  V).

finger are obviously dependent on  $\delta$ . Furthermore, the distribution of  $d_{lev}$  and  $\varepsilon_{max}$  under diverse values of  $\delta$  and  $g_2$  are also shown in Figs. 10 and 11, if the value of  $V_p$  is still 20 V and the  $g_1$  is confined to 2.0  $\mu\text{m}$ . Results show that the values of  $d_{lev}$  and  $\varepsilon_{max}$  become more predominant as the value of  $g_2$  decreases, and the structural responses of movable finger are also obviously dependent on  $\delta$ . By the same token, to tune up the value of  $g_2$  is more useful for levitation control of MEMS comb drive design because the effect of variations in  $g_2$  on  $d_{lev}$  and  $\varepsilon_{max}$  are larger than that of  $g_1$ .

#### 4. Discussions

- (1) Although it is essential that both movable and fixed fingers of a comb drive remain coplanar for high quality MEMS devices, it was also reported that 2  $\mu\text{m}$ -thick polysilicon resonators with compliant folded-beam suspensions have been observed to levitate over 2  $\mu\text{m}$  when driven by an electrostatic comb biased with a DC voltage of 30 V [2]. Therefore, it is important to obtain an accurate electrostatic and structural response of the movable fingers.
- (2) After using FEM to accurately calculate the electrostatic response of the comb finger biased with a DC voltage, the induced vertical force per unit length of the movable comb finger can be obtained. Once the value of levitating force density is obtained, the levitation of the movable fingers under diverse distances traveled can be easily calculated. By way of FEM, accurate value for electrostatic and mechanical fields, considering the variable gaps between fingers, and from fingers to the ground plane, can be obtained.
- (3) Generally, the values of normal electric field intensity ( $E_{n,1}$ ) on the bottom and on the upper side of movable finger  $E_{n,2}$  are obviously dependent on the value of the location to the left side of movable finger ( $loc_y$ ) as shown in Fig. 2. In addition, the value of  $E_{n,2}$  is higher than that of  $E_{n,1}$  because the electric potential gradients, and the values of  $E_n$  near the right and left sides are much higher than those over other regions of the movable fingers due to fringing effects.
- (4) From the results of this article, one can see that the levitating displacement  $d_{lev}$  and strain  $\varepsilon_{max}$  of the movable fingers are

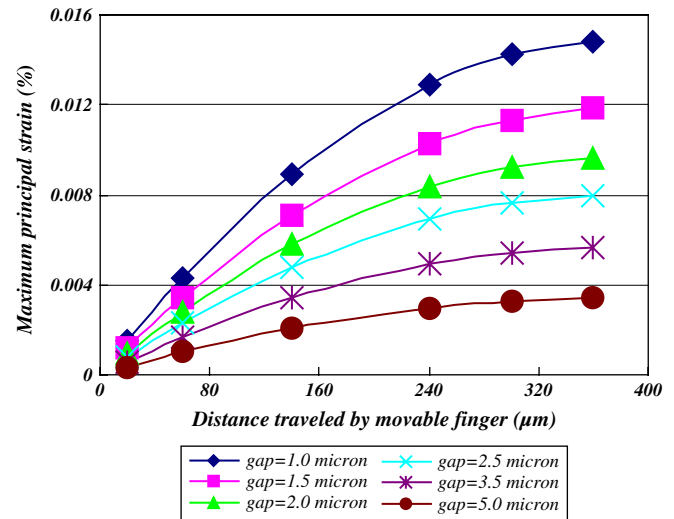


**Fig. 11.** The distribution of maximum principal strain under diverse distances traveled by movable finger and gaps between movable and fixed fingers ( $V_p = 20$  V).

dependent on the traveled distance ( $\delta$ ). The smaller the gap between comb drive fingers and ground plane ( $g_1$ ), the larger the structural response of the movable finger. In addition, levitation also becomes more predominant as the gap between movable and fixed fingers ( $g_2$ ) decreases.

#### 5. Conclusions

An elaborate and extensive electrostatic and structural analysis of an MEMS comb drive, considering the effects of gaps and traveled distance, was efficiently carried out using FEM. Results show that the levitation response of movable finger is apparently dependent on gap size of the MEMS comb drive, and the effect of variations in the gap between movable and fixed fingers on levitation is larger than the gap between the comb drive fingers and the ground plane.

#### References

- [1] W.C. Tang, T.C.H. Nguyen, M.W. Judy, R.T. Howe, Lateral driven polysilicon resonant microstructures, *Sensor. Actuat.* 20 (1989) 25–32.
- [2] W.C. Tang, T.C.H. Nguyen, M.W. Judy, R.T. Howe, Electrostatic-comb drive of lateral polysilicon resonators, *Sensor. Actuat.* A21–23 (1990) 328–331.
- [3] W.C. Tang, M.G. Lim, R.T. Howe, Electrostatic comb drive levitation and control method, *IEEE J. Microelectromech. Syst.* 1 (4) (1992) 170–178.
- [4] J.L.A. Yeh, C.Y. Hui, N.C. Tien, Electrostatic model for an asymmetric comb drive, *IEEE J. Microelectromech. Syst.* 9 (1) (2000) 126–135.
- [5] S.W. Chyuan, Y.S. Liao, J.T. Chen, Computational study of the effect of finger width and aspect ratios for the electrostatic levitating force of MEMS comb drive, *IEEE J. Microelectromech. Syst.* 14 (2) (2005) 305–312.
- [6] M.N.O. Sadiku, *Numerical Techniques in Electromagnetics*, CRC Press, Inc., 1992.
- [7] M.V.K. Chari, S.J. Salon, *Numerical Methods in Electromagnetism*, Academic Press, 2000.
- [8] O.C. Zienkiewicz, K. Morgan, *Finite Elements and Approximation*, Pineridge Press, 1983.
- [9] J. Jin, *The Finite Element Method in Electromagnetics*, John Wiley & Sons, Inc., 2002.
- [10] S.W. Chyuan, Y.S. Liao, J.T. Chen, An efficient method for solving electrostatic problems, *IEEE Comput. Sci. Eng. Magn.* (2003) 52–58.
- [11] S.W. Chyuan, Y.S. Liao, J.T. Chen, Efficient techniques for BEM rank-deficiency electrostatic problems, *J. Electrostat.* 66 (2008) 8–15.